

Article

Optimal Scheduling of a Cascade Hydropower Energy Storage System for Solar and Wind Energy Accommodation

Yuanyuan Liu ¹, Hao Zhang ^{1,2,*}, Pengcheng Guo ^{1,2,*} , Chenxi Li ² and Shuai Wu ²

¹ School of Water Resources and Hydro-Electric Engineering, Xi'an University of Technology, Xi'an 710048, China

² State Key Laboratory of Eco-Hydraulics in Northwest Arid Region, Xi'an University of Technology, Xi'an 710048, China

* Correspondence: hzhang@xaut.edu.cn (H.Z.); guoyicheng@xaut.edu.cn (P.G.)

Abstract: The massive grid integration of renewable energy necessitates frequent and rapid response of hydropower output, which has brought enormous challenges to the hydropower operation and new opportunities for hydropower development. To investigate feasible solutions for complementary systems to cope with the energy transition in the context of the constantly changing role of the hydropower plant and the rapid evolution of wind and solar power, the short-term coordinated scheduling model is developed for the wind–solar–hydro hybrid pumped storage (WSHPS) system with peak shaving operation. The effects of different reservoir inflow conditions, different wind and solar power forecast output, and installed capacity of pumping station on the performance of WSHPS system are analyzed. The results show that compared with the wind–solar–hydro hybrid (WSH) system, the total power generation of the WSHPS system in the dry, normal, and wet year increased by 10.69%, 11.40%, and 11.27% respectively. The solar curtailment decreased by 68.97%, 61.61%, and 48.43%, respectively, and the wind curtailment decreased by 76.14%, 58.48%, and 50.91%, respectively. The high proportion of wind and solar energy connected to the grid in summer leads to large net load fluctuations and serious energy curtailment. The increase in the installed capacity of the pumping station will promote the consumption of wind and solar energy in the WSHPS system. The model proposed in this paper can improve the operational flexibility of hydropower station and promote the consumption of wind and solar energy, which provides a reference for the research of cascade hydropower energy storage system.

Keywords: multi-energy hybrid generation; wind and solar power; cascade hydropower stations; complex hydraulic coupling; pumping station; water energy storage



Citation: Liu, Y.; Zhang, H.; Guo, P.; Li, C.; Wu, S. Optimal Scheduling of a Cascade Hydropower Energy Storage System for Solar and Wind Energy Accommodation. *Energies* **2024**, *17*, 2734. <https://doi.org/10.3390/en17112734>

Academic Editor: Alban Kuriqi

Received: 11 April 2024

Revised: 21 May 2024

Accepted: 1 June 2024

Published: 4 June 2024



Copyright: © 2024 by the authors. Licensee MDPI, Basel, Switzerland. This article is an open access article distributed under the terms and conditions of the Creative Commons Attribution (CC BY) license (<https://creativecommons.org/licenses/by/4.0/>).

1. Introduction

To meet the growing demand for energy, actively promoting the evolution of renewable energy has turned out to be a crucial energy strategy [1–3]. The total installed capacity of renewable energy already reached 1161 GW in China, with 393 GW of solar power and 366 GW of wind power by the end of 2022. The renewable energy integrated power grid exemplified by wind power and solar power provides a new solution to solve energy problems [4–6]. The problem of renewable energy curtailment is caused by the mismatch between power generation characteristics and power demand, the power structure of insufficient peak load storage, the construction of transmission network channels, and the power market. To adapt to the continuous increase proportion of new energy in the power system, research on the multi-energy scheduling optimization power generation technology has important scientific and engineering application value [7–9].

Faced with a significant influx of new energy sources, the challenge of managing the erratic nature of short-term wind and solar energy production has emerged as a focal point in hydropower dispatching studies lately [10–12]. Hydropower, as a clean energy with

excellent regulatory performance, has flexible and rapid peak shaving capacity, which can fully compensate the randomness, volatility, and intermittence of solar and wind energy [13,14]. At the end of 2022, the hydropower plant installed capacity exceeded 413 GW in China, ranking first in the world, with most of them being large-scale cascade hydropower stations. Based on the analysis of installed capacity and technical reliability of hydropower, the conventional hydropower station is considered the most reliable and flexible resource now [15–17].

With a high proportion of solar and wind integrated grids, hydropower needs to adjust output power frequently to match fluctuations in solar and wind output. The optimization scheduling of the hybrid system not only requires thinking about the characteristics of wind and solar output, but also needs to fully take into account the complex operational constraints of hydropower plant. How to achieve the cooperative and complementary optimal dispatch of hydropower stations with wind and solar power output, as well as the reliable, safe, and economic operation of the power grid, is also the focus of attention for researchers at home and abroad. There have been numerous explorations into characterizing the uncertainties surrounding wind and solar energy. Zhang et al. presented a multi-objective operational model for the WSH system, taking into account uncertainty conditions [18]. Tan et al. developed an optimal real-time load distribution model for WSH systems based on uncertainty in wind and solar power generation forecasts [19]. Shi et al. described wind power prediction errors through an uncertainty model, and established a complementary operation model of wind-water-thermal system [20]. Liao et al. modeled the uncertainty of wind and solar output and proposed a short-term peaking model for hydraulic-wind-solar systems [21]. Huang et al. considered coupling the prediction uncertainty and proposed a three-stage optimal dispatch model [22]. Jiang et al. established a short-term optimal scheduling model for a multi-energy complementary system, considering the output forecasting errors of wind and solar power [23].

Most of the existing studies on the optimization of multi-energy complementary operation focus on short-term scheduling, and hydropower plays the role of peak regulation. In addition to uncertainty characterization, it also includes complementary scheduling modeling and efficient solution of scheduling models. Xie et al. investigated a optimal dispatch model for a cascade hydropower WSH system considering hydropower rotation and regulation reserve [24]. Huang et al. presented three risk factors to analyze the problems existing in the optimized scheduling of the WSH system [25]. Shu et al. investigated a peaking strategy to minimize residual load variance [26]. Li et al. presented an optimal operational model with the aim of minimizing the total power generation of the system, minimizing the ecological over-short of discharge, and minimizing the monthly combined output over the whole dispatching cycle [27]. Zhang et al. established a coordinated dispatch operational model for wind-solar-hydro-thermal hybrid power production systems that takes into account the dynamic frequency response [28]. Liu et al. established a coordinated optimal operational model for a WSH system with opportunity based constraints to achieve the peak shaving and ensure maximum power production [29]. Tan et al. presented a coordinated operational model of WSH system that considers operational costs and risks [30]. Wang et al. presented a wind-solar-hydro-thermal coordinated scheduling model considering the integration pumped-storage hydropower [31]. Zhang et al. analyzed the ability of a mixed system including hydropower, solar power, and wind power to match the source and load within an ultra-short-term period [32]. Guo et al. presented a novel hybrid time-steps short-term optimal dispatch model with the assistance of artificial intelligence [33]. The research focused on the analysis of complementary operation of hybrid generation systems, and the safe and stable operation of power grids. The essence of a WSH system complementary operation is to give play to the good adjustment capacity of hydropower plant to promote the consumption of random wind and solar output.

However, in the above optimal scheduling model, cascade hydropower is still mainly power generation, supplemented by adjusting the volatility and randomness of wind and solar energy. Considering the expected proportion of future wind and solar energy

generation, the inherent volatility and uncontrollability of wind and solar energy are also amplified, and the above model is no longer suitable for the expanding wind and solar energy installed capacity industry prospects. Therefore, some hydropower should be changed from the conventional power generation to the regulator, taking into account the role of power generation and energy storage. Pumped storage and hydropower stations with reservoirs are the prevalent methods of energy storage, offering dual benefits of serving as power sources for power grids and mitigating the intermittency of renewable energy. AK et al. studied the transformation of a traditional cascade hydropower station into a cascade pumped storage by substituting the existing turbine with a pump as turbine [34]. Another way is to install a pumping station and diversion pipeline on the basis of the conventional hydropower plant and transform it into a pumped storage plant, which requires a large amount of capital investment while being limited by the construction site [35,36]. By using the existing reservoirs, the problems of the lack of suitable locations for the construction of pumped storage plants and the impact on the ecological environment can be solved. It is a new idea to build cascade hydropower energy storage by using cascade hydropower stations, which can consume wind power and solar power output to a greater extent, and fully tap hydropower potential. Zhang et al. assessed the possibility of converting cascade hydropower plants into a cascade hydropower energy storage system by constructing additional pumping stations between two nearby reservoirs [37]. Wang et al. investigated the synergistic functioning of pumped storage–wind–photovoltaic hybrid systems across various temporal intervals, evaluating the financial advantages and energy performance of the integrated systems [38]. Ju et al. established a two-stage robust unit combination model for cascade water energy storage wind and wind, taking into account the uncertainty of new energy sources [39]. The research on the transformation of cascade hydropower station into pumped storage system has obtained preliminary results. However, the complementary operation and day-ahead optimal scheduling of a cascade energy storage system and wind and solar energy are mostly based on hydropower stations. This approach lacks engineering application-level optimization models with smaller time scales, failing to fully demonstrate the flexibility of power system regulation.

The complementary operation of the cascade hydropower energy storage system is represented in Figure 1. By capitalizing on the discrepancy between the generation of new energy and demand, the pumping station is employed to transfer water flow from downstream to the higher reservoir during times of excess new energy production. This surplus energy is then reserved in the water level energy, facilitating the efficient recycling of energy derived from water levels. The purpose of this paper is to improve the flexibility of cascade hydropower stations, maximize the total power generation of the WSHP system, minimize the renewable energy curtailment, and minimize the net load fluctuation. Considering the combination of hydropower unit and water pump, a multi-objective intra-day scheduling model with 15-min scheduling interval is established. The model fully considers the hydraulic connection between the cascade hydropower stations, the changes in turbine and pump operating conditions, as well as starting, closing, and other constraints. It has also introduced vibration zones for the operation of hydropower units to mitigate the negative impact of renewable energy variability on the system, in order to consume wind and solar power to a greater extent, and fully tap hydropower potential. This method is more suitable for the actual operation of the complementary system, which can provide a reference for the application research of cascade hydropower energy storage engineering.

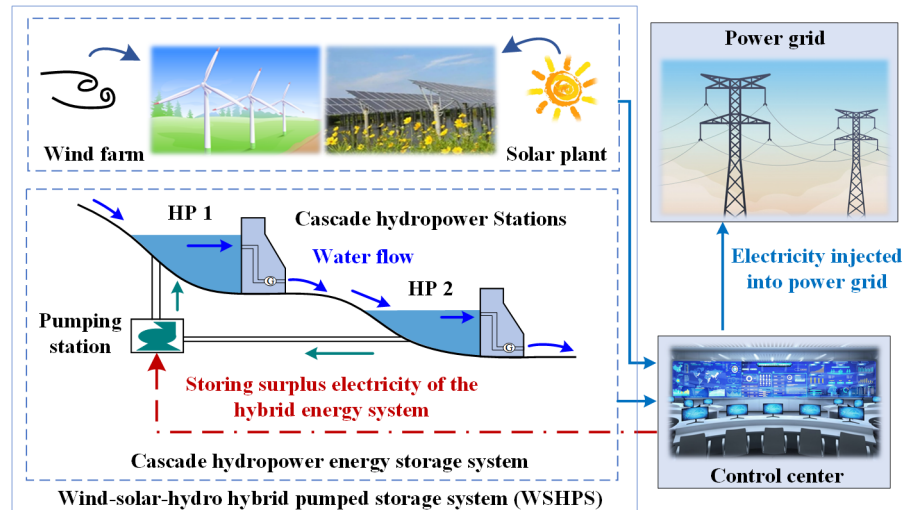


Figure 1. Hybrid generation system schematic diagram of a cascade hydropower energy storage system.

2. Cascade Hydropower Energy Storage System Optimal Scheduling Model

The massive integration of wind and solar energy into the grid has increased system volatility and affected the reliability of grid operation, especially peak shaving. The mismatch between renewable energy generation characteristics and electricity demand, the insufficient power structure for peak power storage, and the restriction of power grid transmission channel results in frequent new energy output curtailment. The WSHPS system is a reform of the WSH system that includes a pumping station, resulting in significant changes to the operation of the hybrid system. Pumping stations have the capability to transform surplus electrical power into potential energy for water when solar and wind power surpass the transmission capacity threshold. The integrated wind–solar–hydro operation offers a new pathway to make up for the unsteadiness of wind and solar power. This approach can contribute to the stabilization of wind and solar energy provision and decrease energy curtailment. The flowchart of complementary wind and solar energy generation using cascade hydropower energy storage is shown in Figure 2.

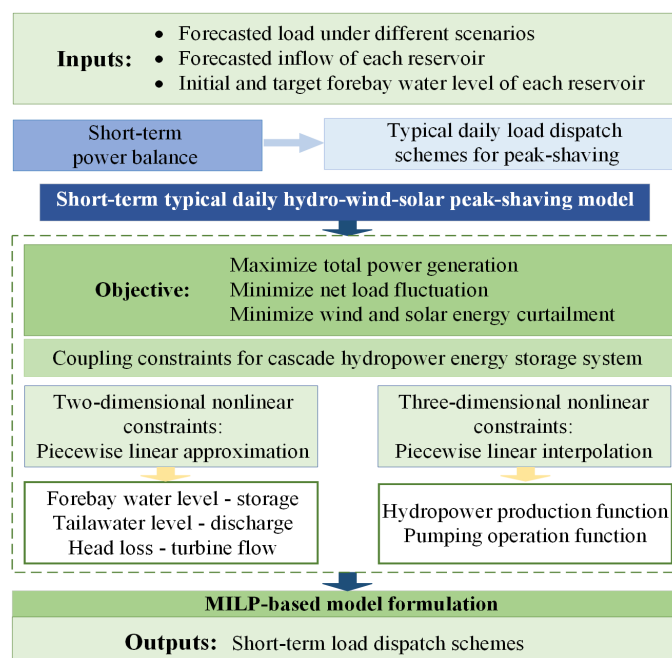


Figure 2. Flowchart of optimal scheduling using cascade hydropower energy storage to complement wind and solar output.

2.1. Operational Modeling

The primary target of optimal operation in the WSHPS system is to effectively utilize the regulating capabilities of the hydropower plant to increase the power output of the integrated system. This involves ensuring a more stable net load, maximizing the output from wind and solar energy, and minimizing the need for frequent adjustments to hydropower output. In order to maximize the performance of hydropower station peak shaving and assure the security and reliable operation, the objective of this model is to maximize the total power generation of the complementary system, minimize wind and solar energy curtailment, and minimize the net load fluctuations. The comprehensive optimization objective is established as follows:

$$\min F = k_1 f_1 + k_2 f_2 + k_3 f_3 \quad (1)$$

1. Maximizing total power generation

In the assessment of the advantages of the hybrid power generation system, the primary consideration is the electricity generation:

$$\max f_1 = \sum_{t=1}^T (P_t^H + P_t^W + P_t^{PV}) \times \Delta t \quad (2)$$

2. Minimizing wind and solar energy curtailment

The efficiency of solar and wind energy consumption during the dispatch period is measured by cumulative wind and solar energy curtailment:

$$\min f_2 = \sum_{t=1}^T (P_t^{W,C} + P_t^{PV,C}) \times \Delta t \quad (3)$$

3. Minimizing net load fluctuation

The net load of the system refers to the effective power of the hydropower, which is calculated by subtracting the coupled power of wind and solar energy from the system load demand:

$$\begin{aligned} \min f_3 &= \frac{1}{T} \sum_{t=1}^T |P_{nt} - P_{av}| \\ P_{nt} &= P_t^{Load} - P_t^W - P_t^{PV} \\ P_{av} &= \frac{1}{T} \sum_{t=1}^T P_{nt} \end{aligned} \quad (4)$$

2.2. Models for Calculating the Hybrid System

2.2.1. Wind and Solar Power Model

When the wind passes through the blades, the wind energy is not fully utilized, and only part of the energy is converted into the mechanical energy for the blades. The wind power output is contingent upon wind speed [40]. The output of solar power station is obtained by analyzing the operational data of solar power stations in the vicinity of hydropower plants or by calculating it using meteorological data [38]:

$$P_t^W = \begin{cases} 0 & 0 \leq V_t \leq V_i \\ \frac{1}{2} C_p A \rho V_t^3 & V_i \leq V_t \leq V_r \\ P_e & V_r \leq V_t \leq V_o \\ 0 & V_o \leq V_t \end{cases} \quad (5)$$

$$P_t^{PV} = \frac{R_t}{1000} [1 + \lambda (T_t - T_{cref})] N_s \quad (6)$$

$$R_t = R_{s,t} \sin(\alpha_x + \beta_x - \varepsilon) \quad (7)$$

2.2.2. Hydropower Model

The nonlinear function of the turbine flow and head can represent the hydropower output:

$$P_{i,n,t} = f_{i,n}^H(Q_{i,n,t}, H_{i,n,t}) \quad (8)$$

2.2.3. Pumping Station Model

The pumping station model has the capability to transform electrical energy into the water level potential energy. The pumped electricity consumption during the period of t can be calculated as:

$$P_{m,t} = f_m^P(Q_{m,t}, H_{m,t}) \quad (9)$$

2.3. Constraints

2.3.1. The Power Balance Constraint

The power balance constraint guarantees the combined generation from wind, solar, pumping station, and cascade hydropower is sufficient to meet the electricity demand:

$$P_t^W + P_t^{PV} + P_t^H + P_t^P = P_t^{Load} \quad (10)$$

2.3.2. Wind and Solar Power Constraint

$$0 \leq P_t^W \leq P^{W \max} \quad (11)$$

$$0 \leq P_t^{PV} \leq P^{PV \max} \quad (12)$$

2.3.3. Cascade Hydropower Constraints

1. Water balance constraints

The reservoir water balance for the WSHPS system is influenced by the pumping flow:

$$V_{ur,t} = V_{ur,t-1} + 3600 \cdot (I_{ur,t} + Q_t^P - Q_{ur,t}^p - Q_{ur,t}^d) \Delta t, \{ur\} \in I \quad (13)$$

$$V_{lr,t} = V_{lr,t-1} + 3600 \cdot (I_{lr,t} - Q_t^P - Q_{ur,t}^p - Q_{ur,t}^d) \Delta t, \{lr\} \in I \quad (14)$$

$$V_{i,t} = V_{i,t-1} + 3600 \cdot (I_{i,t} - Q_{i,t}^p - Q_{i,t}^d) \Delta t \quad (15)$$

2. Cascade hydropower plant reservoir hydraulic connection

The total reservoir inflow of hydropower plant i can be shown as:

$$I_{i,t} = Q_{i-1,t-\tau} + R_{i,t} \quad (16)$$

3. Reservoir forebay water level constraints

$$Z_i^{up,\min} < Z_{i,t}^{up} < Z_i^{up,\max} \quad (17)$$

4. Forebay water level constraints

When determining the reservoir operation, it is essential to take into account the sustainability of water resources and the reservoir reserve needs of the hydropower station at the end of the operational period in order to fulfill the water consumption objectives:

$$Z_{i,1}^{up} = Z_{i,begin}^{up} \quad (18)$$

$$Z_{i,end}^{up} - \delta \leq Z_{i,T}^{up} \leq Z_{i,end}^{up} + \delta \quad (19)$$

5. Total discharge constraints

In terms of water supply and ecological flow, the total discharge from reservoirs is constrained by both upper and lower limits:

$$\begin{aligned} Q_i^{\min} &< Q_{i,t} < Q_i^{\max} \\ Q_{i,t} &= Q_{i,t}^p + Q_{i,t}^d \end{aligned} \quad (20)$$

6. Hydropower output constraints

$$P_i^{\min} \leq P_{i,t} \leq P_i^{\max} \quad (21)$$

7. Relationship between capacity and reservoir water level

$$V_{i,t} = f_i^{zv}(Z_{i,t}^{up}) \quad (22)$$

8. Relationship between tailwater level and discharge flow

$$Z_{i,t}^{down} = f_i^{zq}(Q_{i,t}) \quad (23)$$

2.3.4. Hydropower Individual Unit Constraints

1. Unit output constraints

$$u_{i,n,t} P_{i,n}^{\min} \leq P_{i,n,t} \leq u_{i,n,t} P_{i,n}^{\max} \quad (24)$$

$$P_{i,t} = \sum_{n=1}^N u_{i,n,t} P_{i,n,t} \quad (25)$$

2. Hydropower unit generation flow constraints

$$u_{i,n,t} Q_{i,n}^{\min} \leq Q_{i,n,t} \leq u_{i,n,t} Q_{i,n}^{\max} \quad (26)$$

$$Q_{i,t}^p = \sum_{n=1}^N u_{i,n,t} Q_{i,n,t} \quad (27)$$

3. Constraints on vibration zones

Hydropower units contain several prohibited operating zones (or vibration zones), and it should be prevented from operating in the vibration area as far as possible:

$$(P_{i,n,t} - P_{i,n,k}^{\max})(P_{i,n,t} - P_{i,n,k}^{\min}) \geq 0 \quad (28)$$

4. Constraints on online and offline duration

$$\begin{cases} u_{i,n,t} - u_{i,n,t-1} = y_{i,n,t}^{\text{on}} - y_{i,n,t}^{\text{off}} \\ y_{i,n,t}^{\text{on}} + y_{i,n,t}^{\text{off}} \leq 1 \end{cases} \quad (29)$$

$$\begin{cases} y_{i,n,t}^{\text{on}} + \sum_{\lambda=t+1}^{t+T_{i,n}^{\text{on}}-1} y_{i,n,\lambda}^{\text{off}} \leq 1 \\ y_{i,n,t}^{\text{off}} + \sum_{\lambda=t+1}^{t+T_{i,n}^{\text{off}}-1} y_{i,n,\lambda}^{\text{on}} \leq 1 \\ \sum_{t=1}^T y_{i,n,t}^{\text{on}} \leq M_{i,n}^{\text{on}} \end{cases} \quad (30)$$

5. Power climbing constraint of hydropower unit

$$-\Delta P_{i,n} \leq P_{i,n,t+1} - P_{i,n,t} \leq \Delta P_{i,n} \quad (31)$$

6. Power fluctuation constraint of hydropower unit

$$\begin{aligned} (P_{i,n,t} - P_{i,n,t-\sigma-1})(P_{i,n,t} - P_{i,n,t-1}) \geq 0 \\ \sigma = 1, 2, \dots, t_e - 1 \end{aligned} \quad (32)$$

7. Hydropower unit generating head constraints

$$H_{i,n,t} = \frac{Z_{i,t}^{\text{up}} - Z_{i,t-1}^{\text{up}}}{2} - Z_{i,t}^{\text{down}} - H_{i,n,t}^{\text{loss}} \quad (33)$$

8. Head loss function

$$H_{i,n,t}^{\text{loss}} = f_{i,n}^{HQ}(Q_{i,n,t}^P) \quad (34)$$

2.3.5. Pumping Station Constraints

1. Pump power constraints

$$P_{m,t} = u_{m,t} P_m^{\text{Pr}} \quad (35)$$

$$P_t^P = \sum_{m=1}^M u_{m,t} P_{m,t} \quad (36)$$

2. Pump flow constraints

$$u_{m,t} Q_m^{\text{min}} \leq Q_{m,t} \leq u_{m,t} Q_m^{\text{max}} \quad (37)$$

$$Q_t^P = \sum_{m=1}^M u_{m,t} Q_{m,t} \quad (38)$$

3. Pump operating head constraints

$$H_{m,t} = Z_{i,t}^{\text{up}} - Z_{i+1,t}^{\text{up}} \quad (39)$$

2.4. Linearization of Nonlinear Constraints

With the advantages of a flexible modeling language, an economical and applicable software environment, and efficient global search capability, mixed-integer linear programming (MILP) is widely used in hydropower operation optimization solution. The model presented in the paper includes complex nonlinear constraints that are challenging to solve directly. The nonlinear constraints of the model include Equations (8), (9), (22), (23), (28), (32), (34) and (35). The hydropower station production function, Equation (8), and the pumping station operation function, Equation (9), are primarily nonlinear functions that involve two variables. In this paper, Equations (8) and (9) are linearly approximated using three-dimensional interpolation in the independent branch scheme [41]. For Equations (22), (23), (28), (32), (34) and (35), the piecewise linearization is adopted for linear approximation. By applying the aforementioned linear modeling technique, the initial nonlinear model is transformed into a MILP model, and the model can be resolved easily by the CPLEX solver. The focus of this article is the study of the vibration zone of a individual hydropower unit, a topic that will be explored in depth in the next sections.

In this paper, the linearization method is used to handle Equation (28), as illustrated in Figure 3, assuming that the unit has K prohibited operation zones (POZs). Equations (40) and (41) guarantee that each hydropower unit falls within one of the viable working zones while it is online. Equation (42) guarantees that if $\theta_{i,n,t}^k = 1$, the unit n operating within the k th viable operating region (i.e., $P_{i,n,k-1}^{\max} \leq P_{i,n,t} \leq P_{i,n,k}^{\min}$) [14].

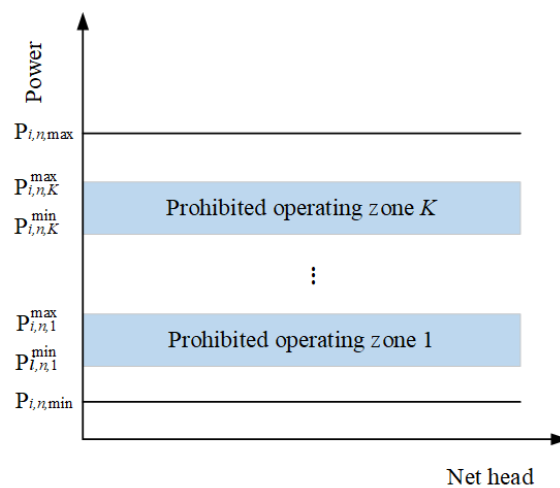


Figure 3. Schematic diagram of multiple prohibited operating zones.

$$\sum_{k=1}^K \theta_{i,n,t}^k = u_{i,n,t} \quad (40)$$

$$\theta_{i,n,t}^k \in \{0, 1\} \quad (41)$$

$$\sum_{k=1}^{K+1} \theta_{i,n,t}^k P_{i,n,k-1}^{\max} \leq P_{i,n,t} \leq \sum_{k=1}^{K+1} \theta_{i,n,t}^k P_{i,n,k}^{\min} \quad (42)$$

3. Case Study

This study focuses on evaluating a combined power generation system comprising a wind farm, two cascade hydropower stations, a solar power station, and a pumping station. The effectiveness of the presented model and methodology is investigated through the abovementioned components. The hydropower station consists of seven independent hydroelectric units, four units in hydropower plant 1 (HP 1) and three units in hydropower plant 2 (HP 2). HP 1 is a multi-year regulated hydropower station located in the upstream of the river and HP 2 is located downstream of HP 1. A pumping station was built between

the HP 1 and HP 2 reservoirs. The water pump adopts three constant speed pump units with a rated power of 100 MW. The parameters of the hydropower stations and reservoirs are given in Table 1, and the characteristic parameters of the hydropower units are given in Table 2.

Table 1. The parameters of the hydropower stations.

Parameters	HP 1	HP 2
Regulating reservoir volume (10^8 m^3)	35	7.2
Dead water level (m)	1071	936
Normal water level (m)	1140	970
Beginning and end water level (m)	1076	950
Beginning and end water level deviation (m)	0.5	0.1
Maximum reservoir release (m^3/s)	6866	12,142
Minimum reservoir release (m^3/s)	180	355
Installed capacity (MW)	900	900
Regulation ability	Multi-year	Daily

Table 2. Operating parameters of hydropower units.

Plant	Unit	$Q_{i,n,max}$ (m^3/s)	$P_{i,n,max}$ (MW)	$P_{i,n,min}$ (MW)	Range of POZs (MW)	$T_{i,n}^{on}/T_{i,n}^{off}$ (h)	t_e (h)
HP 1	#1,2	632.2	250	100	[80 130]	2	1
	#3,4	632.2	200	80	[70 120]	2	1
HP 2	#1–3	490.5	300	150	[130 180]	2	1

The data of wind energy, solar energy, load demand, and residual load on typical days in summer and winter are shown in Figure 4. Figure 5 shows the upstream reservoir inflow scenario of cascade hydropower station constructed in a normal year. The optimization process took into account a planning horizon of 24 h, with each time period lasting 15 min. The model was written with Matlab and solved with CPLEX solver. The criterion for stopping the CPLEX solver is that the final clearance is less than or equal to 0.5%.

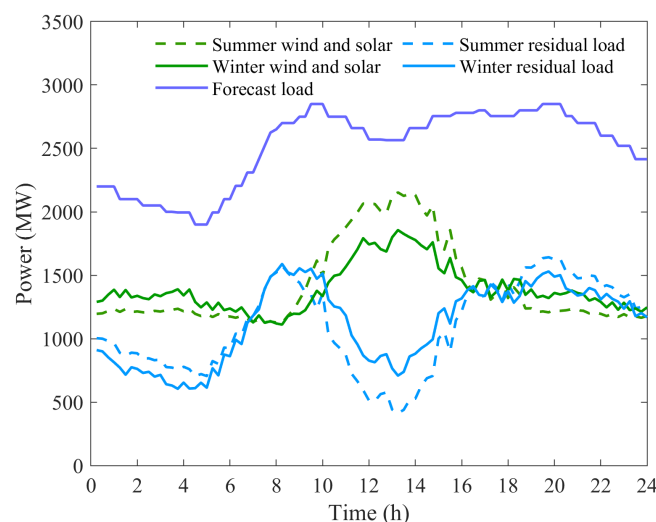


Figure 4. System forecast wind and solar output, residual load, and load demand on typical days in summer and winter.

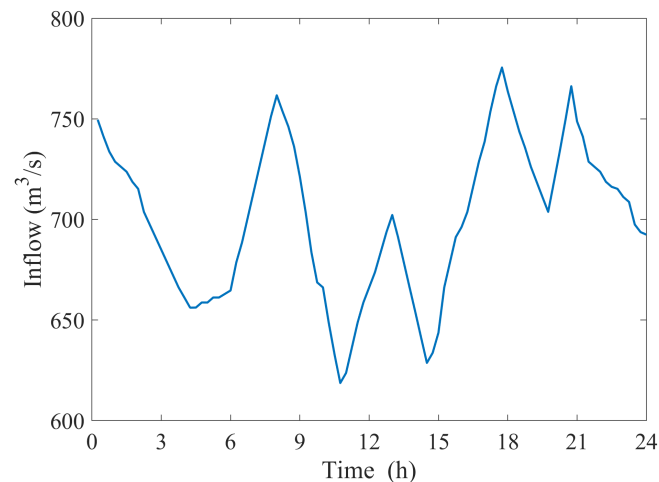


Figure 5. Reservoir inflow of PH 1 in a normal year.

4. Results and Discussion

In order to investigate the reliability and validity of the scheduling model under different operating conditions, the optimization simulation model proposed in Section 2 was studied.

1. The simulation results of WSH and WSHPS systems without pumping station and with pumping station are compared in Section 4.1. The response of different systems to the reservoir inflows of cascade hydropower station is analyzed to demonstrate the advancement of the presented model.
2. The performance of the WSHPS system is compared and analyzed by taking the solar and wind power generation scenarios in summer and winter as reference terms in Section 4.2.
3. The impact of pumping station installation capacity configuration on the complementary scheduling operation of the WSHPS system is studied in Section 4.3.

4.1. Impact of Reservoir Inflows on the Performance for Different Hybrid Systems

The operating processes of two hybrid power generation systems (WSH and WSHPS systems) without and with pumping station were compared. To verify the property and effective of the WSHPS system for dealing with different operating conditions, three reservoir inflow scenarios were chosen to reflect the dry, normal, and wet years, respectively. The reservoir inflow scenarios for dry year ($100 \text{ m}^3/\text{s}$ decrease) and wet year ($100 \text{ m}^3/\text{s}$ increase) were constructed by enlarging the inflow in the normal year, and were used as references for the case study. The optimal operation of the system avoids water overflow as much as possible, so the water spillage is set to 0. Table 3 summarizes the performance of the WSH and WSHPS systems under several typical inflow scenarios.

It can be seen that the WSHPS system can play a role in increasing the total power generation and reducing energy curtailment under different reservoir inflow scenarios. Compared with the WSH system, the total power generation of WSHPS systems increased by 10.69%, 11.40%, and 11.27% in dry, normal, and wet years, respectively. The solar curtailment decreased by 68.97%, 61.61%, and 48.43%, respectively, and the wind curtailment decreased by 76.14%, 58.48%, and 50.91% respectively. In order to maintain the water level balance of the reservoir during the system operation and scheduling period, all the inflow of the upstream reservoir is used for hydropower generation to avoid affecting the amount of water available in the next scheduling period. As the inflow of the upstream reservoir increases, the total power generation of the WSHPS system increases, while the net load volatility of the system decreases and the power consumption of the pumps increases. The increase in hydropower generation squeezes the transmission channels for wind and solar output to a certain extent, leading to a decrease in the consumption capacity of wind and solar energy.

Table 3. The performance of WSH and WSHPS systems under different typical inflows in winter.

Item		Dry Year	Normal Year	Wet Year
Total power generation (MWh)	WSH	60,321.25	60,321.25	60,321.25
	WSHPS	66,771.25	67,196.25	67,121.25
	Increase	10.69%	11.40%	11.27%
Wind curtailment (MWh)	WSH	2201	2502.12	4419.95
	WSHPS	525.16	1038.96	2169.63
	Decrease	76.14 %	58.48%	50.91%
Solar curtailment (MWh)	WSH	474	554.08	897.89
	WSHPS	147.08	212.74	463.03
	Decrease	68.97 %	61.61%	48.43%
Net load fluctuation (MW)	WSH	167.32	153.20	98.19
	WSHPS	257.15	235.49	174.89
Electricity consumption (MWh)	WSHPS	6450	6875	6800

During a normal year in winter, the output processes of each power production unit of the WSH and WSHPS systems are presented in Figure 6. Wind power curtailment is observed during the peak wind power output period of 0:00–6:00, and wind–solar curtailment occurs during the peak solar output period of 11:00–15:00 in the WSH system. Due to the fact that cascade hydropower complements and coordinates fluctuations in the output of wind and solar energy, it helps to promote the consumption of wind and solar energy and improves the efficiency of the complementary system. However, cascade hydropower is limited by natural hydraulic and electrical constraints, and the improvement ability is limited when the power supply support of the grid is prioritized, which inevitably leads to energy curtailment. Similarly, the WSHPS system occurred wind power curtailment during the peak wind power output period of 0:00–6:00, but the curtailment was much smaller compared to the WSH system. During the peak solar output period of 11:00–15:00, there was only a small amount of wind and solar power curtailment. This is due to fact that the pumping station consumes excess wind and solar energy while converting it into hydraulic potential, thus reducing the waste of wind and solar power. From the perspective of output processes, after considering the constraints of unit online and offline, as well as output fluctuation duration, the output of each power station is stable and does not fluctuate frequently. This meets the real operational requirements of the power station, and the power supply support function of the grid is reliable. The output process distributions of two cascade hydropower units during a normal year in winter are represented in Figure 7, and the purple and pink shaded areas represent the prohibited operating zones of HP 1 and HP 2, respectively. The output power of the hydropower unit successfully avoids the prohibited operating zones to meet the requirements of the units climbing ability constraint, ensuring operational safety. Meanwhile, the stable output duration of the unit meets the requirement of the output fluctuation limit constraint (1 h), and the online and offline duration constraint also meets the unit min online and offline duration of 2 h, ensuring the stability of the unit output. Integrating pumping stations can increase the hydropower generation of hybrid systems, and the growth mainly concentrates on HP1. Therefore, the validity of the constraint handling method presented in the paper has been verified. The output power distributions of the WSHPS system during a dry year and wet year in winter are represented in Figure 8. During the flood water period, high inflows into reservoirs increase hydropower production, resulting in a decrease in wind and solar power production and an increase in wind and solar energy curtailment. Figure 9 shows the power consumption process of pumping station units in dry, normal, and wet years.

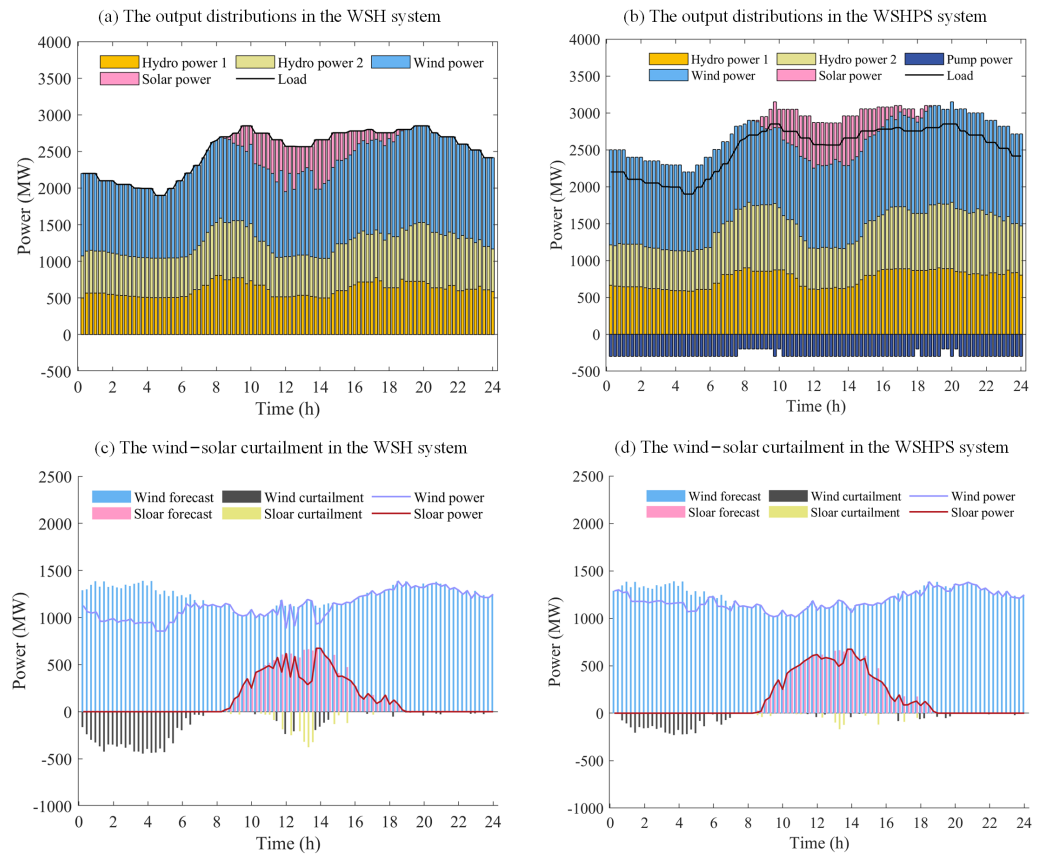


Figure 6. The output distributions and wind-solar curtailment of WSH and WSHPS systems during a normal year in winter.

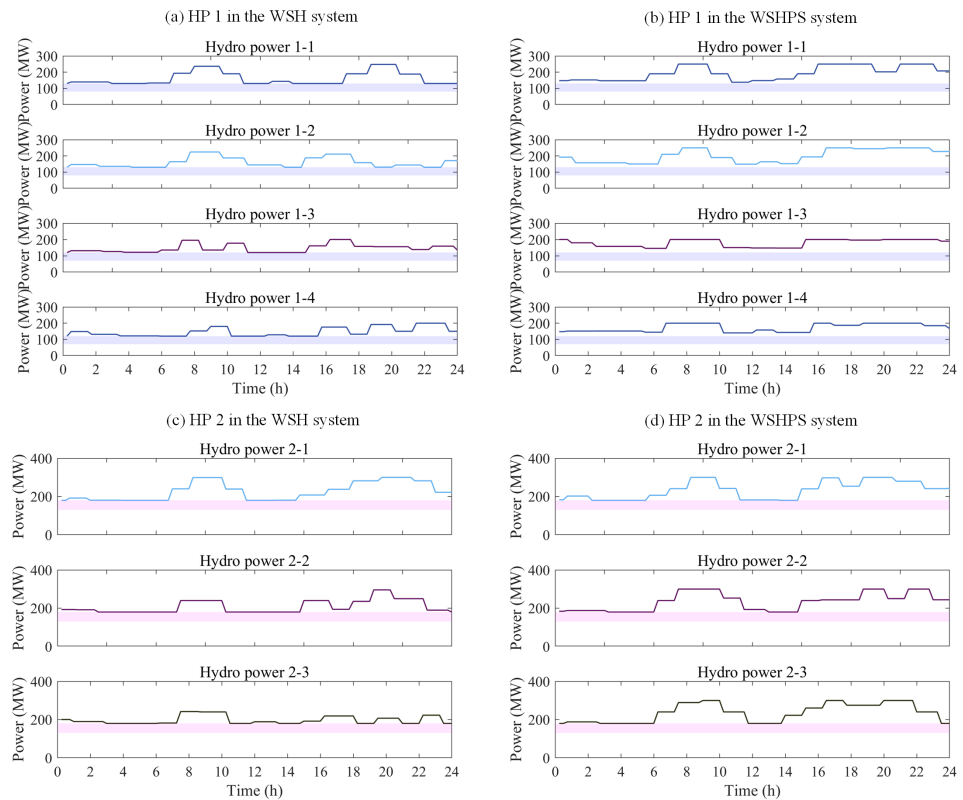


Figure 7. Power generation process of hydropower units of different systems during a normal year in winter.

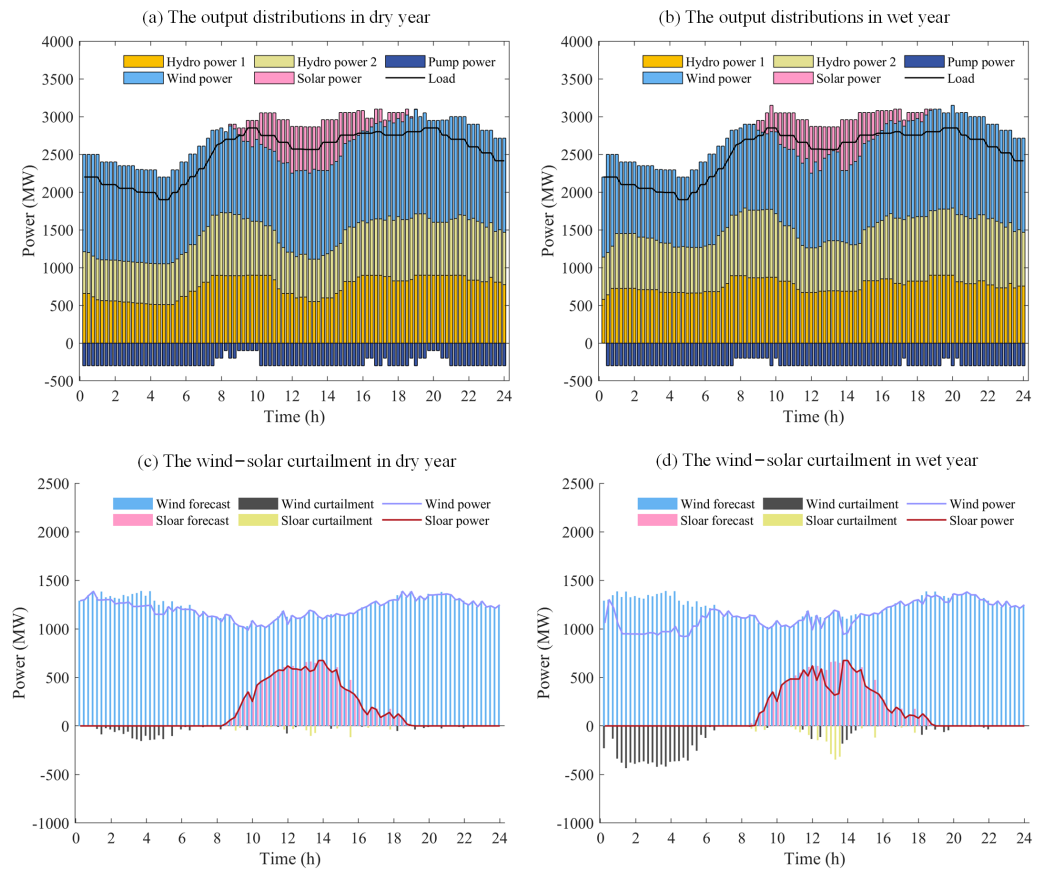


Figure 8. The output distributions and energy curtailment of the WSHPS system during dry and wet years in winter.

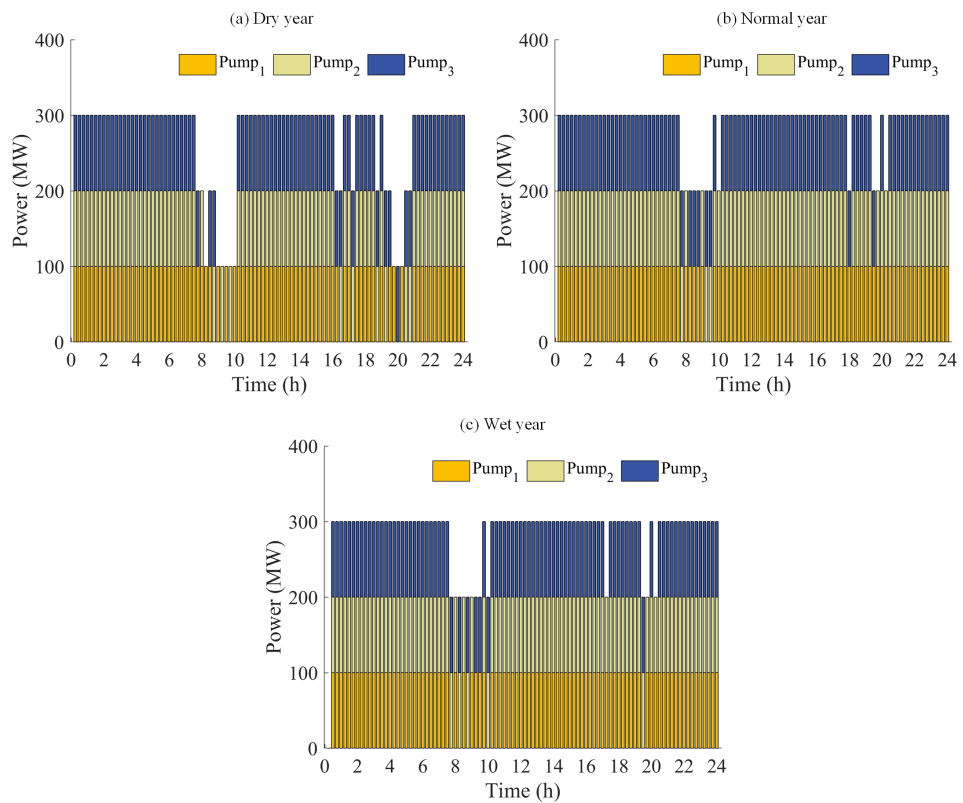


Figure 9. The power consumption process of pumping station units of the WSHPS system in winter.

4.2. Optimal Scheduling of WSHPS System under Different Scenarios

Table 4 summarizes the performance of WSHPS systems under different scenarios in both summer and winter during a normal year. The total power generation of the system is greater in winter than in summer, with a total power generation of 66,996.25 MWh in summer and 67,196.25 MWh in winter, respectively. The fluctuation in net load during summer surpasses that observed in winter, with a net load fluctuation of 264.88 MW in summer and 235.49 MW in winter, respectively. Figure 10 represents the output process distributions of different power generation units, wind–solar energy curtailment, and output processes of hydropower plant units of the WSHPS system during a normal year in summer. Comparing the optimization dispatch results of the WSHPS system in summer and winter, the phenomenon of wind–solar energy curtailment mainly occurs during the peak solar output of period 11:00–15:00 in summer (Figure 10b). As can be obtained from Figure 6d, the wind energy curtailment occurs at the peak of wind power generation during the period 0:00–6:00 and solar power curtailment occurs at the peak of solar output during the period 13:00–14:00 in winter. Because the predicted wind power output in winter is larger, and the predicted solar output in summer is larger, the wind energy curtailment in winter (1038.96 MWh) is higher than in summer (857.21 MWh). The solar power curtailment in summer (747.99 MWh) is greater than that in winter (212.74 MWh). The energy curtailment rates of total wind and solar power in summer and winter are 4.72% and 3.74%, respectively, which can achieve a large amount of consumption of wind and solar energy.

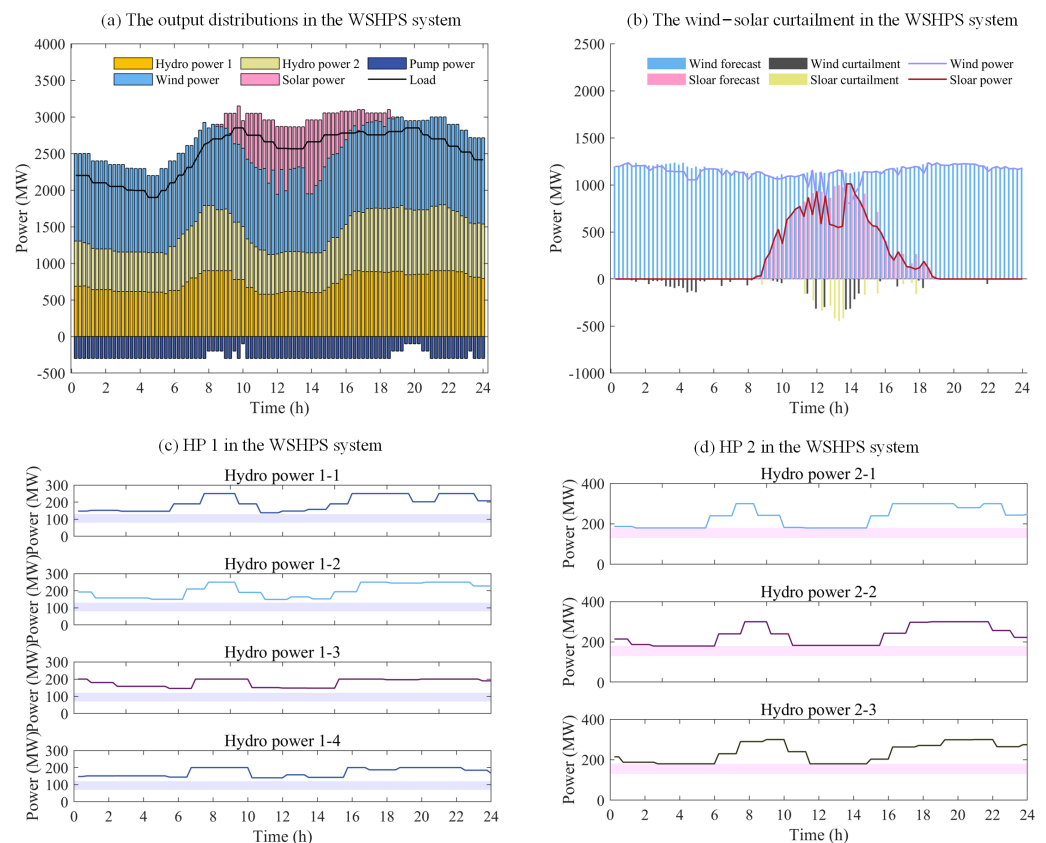


Figure 10. In a normal year, the output distributions, wind–solar curtailment, and power output process of hydropower plant units of the WSHPS system in summer.

Table 4. The performance of WSHPS system under different wind and solar scenarios during a normal year.

Item	Summer	Winter
Total electricity generation (MWh)	66,996.25	67,196.25
Wind curtailment (MWh)	857.21 (3.05%)	1038.96 (3.52%)
Solar curtailment (MWh)	747.99 (12.77%)	212.74 (5.45%)
Net load fluctuation (MW)	264.88	235.49
Electricity consumption (MWh)	6675	6875

4.3. Influence of Installed Capacity Configuration of Pumping Station

Through analyzing the coordinated dispatching mode of WSHPS power generation system with various installed capacity configuration of the pumping station, the influence of installed capacity configuration of the pumping station on the performance of WSHPS system is discussed. Table 5 shows the performance comparison of WSHPS systems under different installed capacities of the pumping station. When the capacity of the pumping station increases, the total electricity generation increases, and the wind and solar power curtailment decreases, accompanied by an increase in the energy consumption of the pump.

Table 5. The performance of WSHPS system with different installed capacity configurations of the pumping station during a normal year in winter.

Item	225 (MW)	300 (MW)	375 (MW)
Total electricity generation (MWh)	65,646.25	67,196.25	68,665
Wind curtailment (MWh)	1265.01 (4.28%)	1038.96 (3.52%)	792.05 (2.68%)
Solar curtailment (MWh)	259.21 (6.64%)	212.74 (5.45%)	181.30 (4.64%)
Net load fluctuation (MW)	219.63	235.49	253.93
Electricity consumption (MWh)	5325	6875	8343.75

The scheduling results for pumping stations with capacities configuration of 225 MW and 375 MW are shown in Figure 11. With a capacity of the pumping station at 225 MW, the output distribution of the WSHPS system power generation unit, as well as the wind–solar energy curtailment distribution, are represented in Figure 11a,c, respectively. The corresponding wind–solar power curtailment is 1524.23 MWh, and the wind and solar energy curtailment rate are 4.28% and 6.64%, respectively. To capture as much wind and solar energy as possible, the pumps run almost 24 h a day under rated conditions. With the growing capacity configuration of the pump, the energy curtailment rate of wind–solar energy decreases. For the pumping station with an installed capacity configuration of 300 MW, the wind and solar energy curtailment rates are 3.52% and 5.45%, respectively. The wind energy and solar energy curtailment rate is 2.68% and 4.64% for the pumping station with an installed capacity configuration of 375 MW.

Figure 12 presented the power output processes of hydropower plant units corresponding to different pumping station installed capacities of the WSHPS system. The output of the hydropower plant units effectively avoids the vibration zones and meets the climbing constraints. Figure 13 depicts the power consumption process of pumping station units with different installed capacities. The power consumption for pumping purposes is recorded as 5325 MW, 6875 MWh, and 8343.75 MWh, respectively, corresponding to the installed capacity configurations of the pumping station, which are 225 MW, 300 MW, and 375 MW. Consequently, the configuration of an additional pumping station will increase the power production of the WSHPS system. Meanwhile, because the fact that pumping stations can consume excess wind–solar energy and convert it into hydraulic potential, it can cut down the wind and solar energy curtailment. However, due to hydropower unit operation constraints, the surplus solar–wind power exceeds the assumed pumping station installed capacity in this case. Therefore, there is still partial wind–solar energy curtailment.

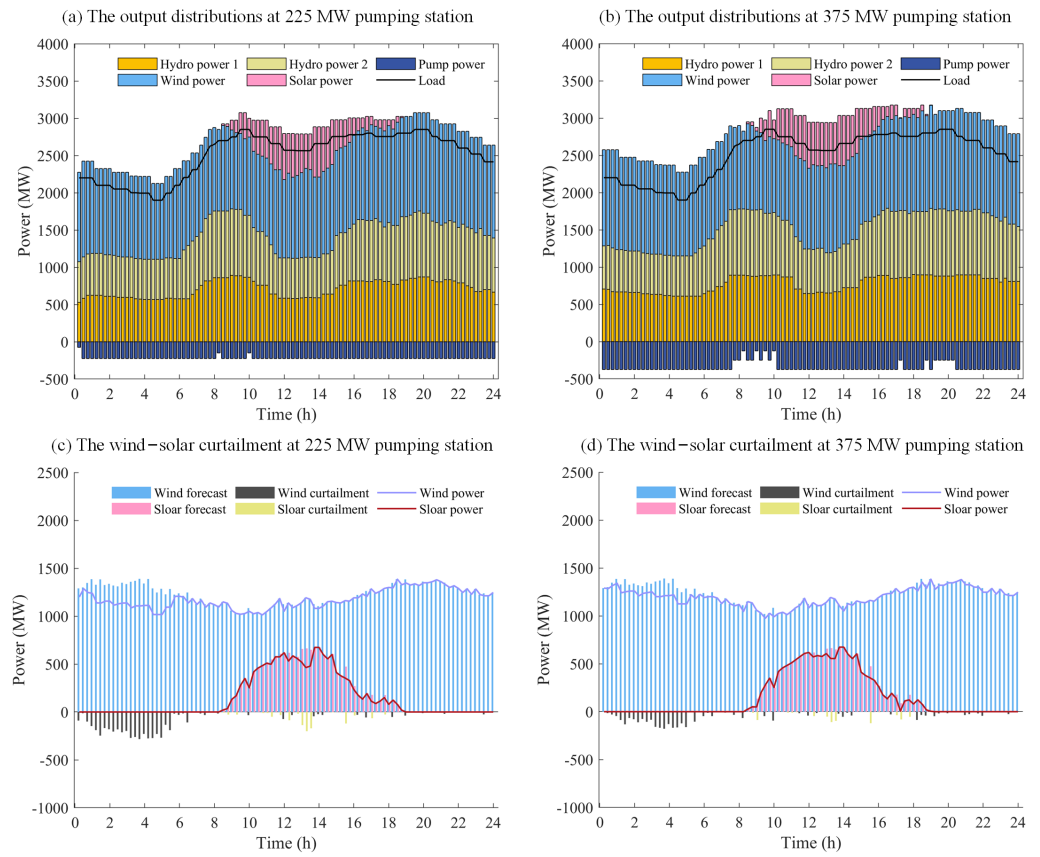


Figure 11. The output distributions of wind-solar curtailment with different installed capacity configurations of the pumping station during a normal year in winter.

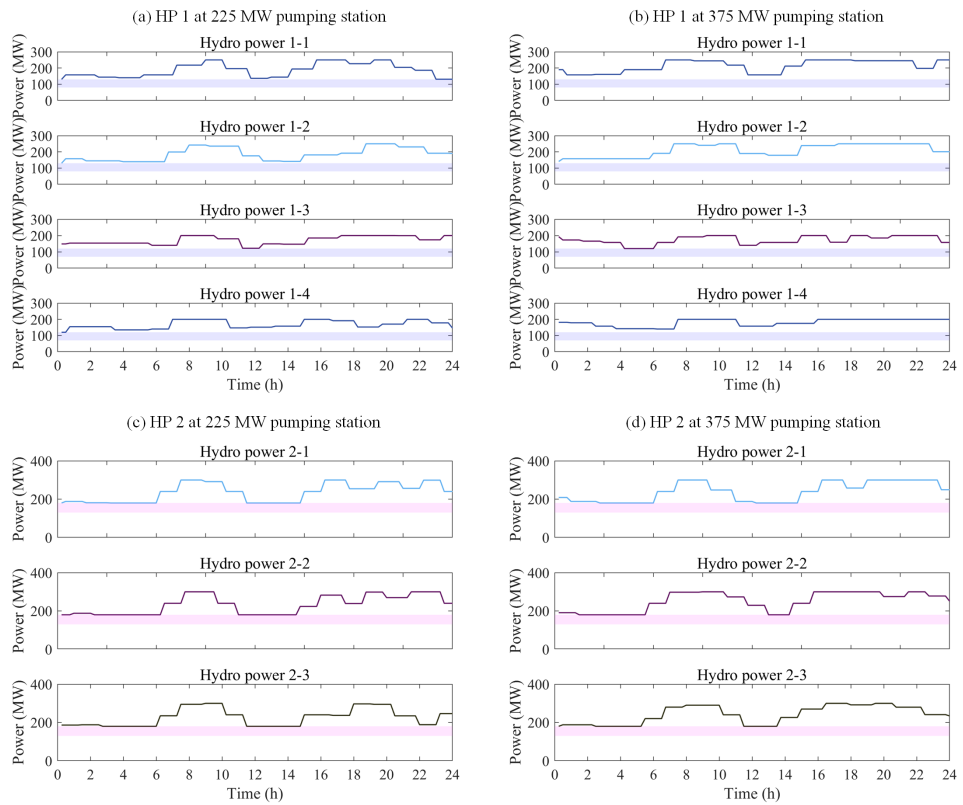


Figure 12. The power output process of hydropower units with different installed capacity configurations of the pumping station during a normal year in winter.

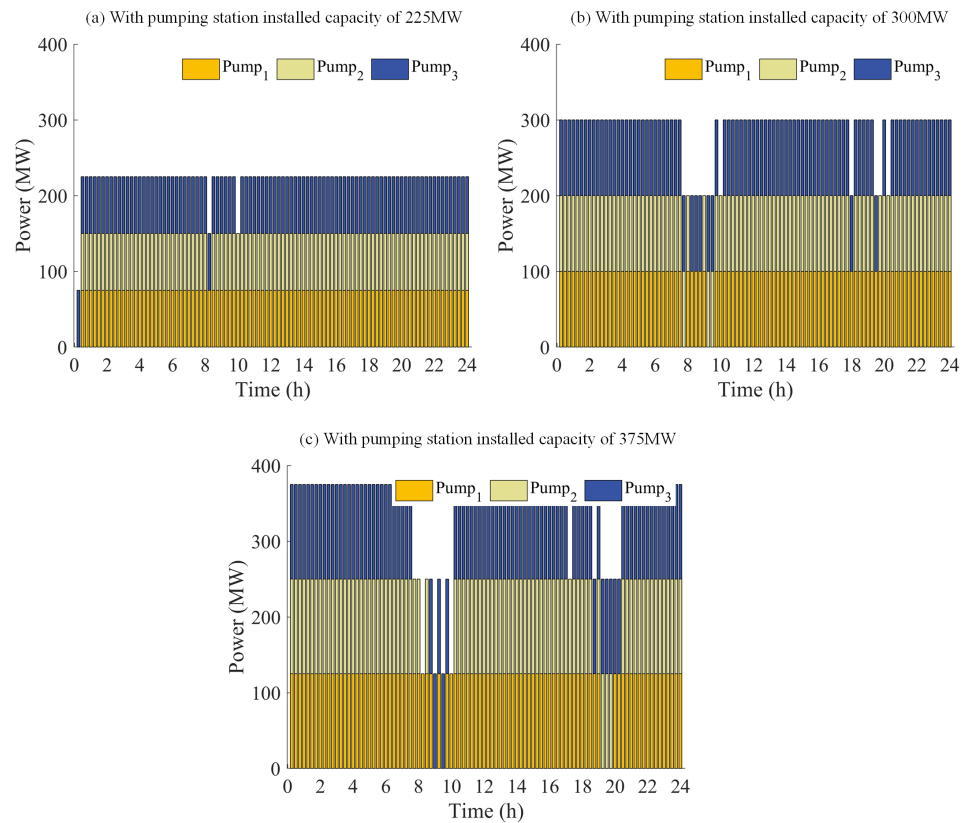


Figure 13. The power consumption process of pump units with different installed capacity configurations of the pumping station during a normal year in winter.

5. Conclusions

In the background of energy transition, the power structure is undergoing changes, and at the same time, the existing methods of multi-energy complementary dispatch also have certain limitations. This paper transforms the function of cascade hydropower plants into a cascade hydropower energy storage system by establishing additional pumping stations between the nearby upstream and downstream reservoirs. Aiming to enhance total power generation, reduce net load fluctuation, and reduce wind and solar energy curtailment, a coordinated optimal model of the WSHPS hybrid system considering the characteristics of multi-energy complementarities is established, and the impact of different factors on the performance of the system are analyzed. The following conclusions can be drawn:

1. The WSHPS system improves total power production and wind–solar energy consumption under different inflow scenarios. Compared with the WSH system, the total power production of WSHPS systems increased by 10.69%, 11.40%, and 11.27% in dry, normal, and wet years, respectively. The solar curtailment decreased by 68.97%, 61.61%, and 48.43%, respectively, and the wind curtailment decreased by 76.14%, 58.48%, and 50.91% respectively.
2. Compared to the scheduling results in winter, the higher proportion of wind and solar integration in summer leads to higher net load fluctuations and serious energy curtailment in summer.
3. As the installed capacity configuration of the pumping stations increases, the total power generation of the WSHPS system increases, while the curtailment of wind and solar energy decreases. However, the energy consumption of the storage pumping stations increases, along with the need for higher construction costs for pumping stations.

By systematically scheduling cascade hydropower stations, solar power plants, wind farms, and energy storage pumping stations, it is possible to maximize the use of com-

plementary energy sources, thereby enhancing the robustness and sustainability of the power supply system. The paper proposes a coordinated control method that combines multiple power generation technologies for large-scale cascade hydropower stations and storage pumping stations. This strategy helps optimize the operational environment of the system, ensuring efficient exploitation of renewable energy and maximizing the flexibility of power regulation.

Author Contributions: Conceptualization, Y.L. and H.Z.; methodology, Y.L.; software, Y.L.; validation, Y.L., C.L. and H.Z.; formal analysis, Y.L. and S.W.; investigation, Y.L.; resources, P.G.; data curation, Y.L.; writing—original draft preparation, Y.L.; writing—review and editing, Y.L., H.Z. and S.W.; visualization, Y.L.; supervision, H.Z. All authors have read and agreed to the published version of the manuscript.

Funding: This research was funded by the National Natural Science Foundation of China (grant numbers 52309119, 51839010); the Fellowship of China National Postdoctoral Program (grant number 2020M683526); the Youth Innovation Team of Shaanxi Universities (grant number 2020-29); and the Innovation Capability Support Program of Shaanxi (Program No. 2024RS-CXTD-31).

Data Availability Statement: The data presented in this study are available on request from the corresponding author.

Conflicts of Interest: The authors declare no conflicts of interest.

Nomenclature

Sets and indices

I	Total number of hydropower plants
i	Index of hydropower plants
k_1, k_2, k_3	Weights associated with each optimization objective
M	Total number of units in the pumping station
m	Index of units in the pumping station
N	Total number of units in the hydropower plant
n	Index of units in the hydropower plant
T	Total number of time periods
t	Index of time periods

Parameters and coefficient

α_x	Latitude of the PV module
β_x	Optimal tilt angle of the PV module
$\Delta P_{i,n}$	Climbing capacity of unit n in plant i [MW]
Δt	Duration of time period t , which is set to 15 min in this paper
δ	Water level deviation at the end of the dispatching period [m]
λ	Temperature coefficient
ρ	Air density [kg/m^3]
ε	Declination angle of the sun
A	Area swept by the wind turbine blade [m^2]
$M_{i,n}^{\text{on}}$	Maximum startup times of the unit n in plant i during the scheduling period
N_s	Rated power of the solar energy [MW]
$P^{\text{PV max}}$	Maximum power output of solar power station [MW]
$P^{\text{W max}}$	Maximum power output of the wind farm [MW]
P_t^{Load}	Load demand of the system in time period t [MW]
$P_{i,n,k}^{\text{max}}$	Upper bound of the k prohibited operating zone of unit n in plant i [MW]
$P_{i,n,k}^{\text{min}}$	Lower bound of the k prohibited operating zone of unit n in plant i [MW]
$P_{i,n}^{\text{max}}$	Maximum power output of unit n in plant i [MW]

$P_{i,n}^{\min}$	Minimum power output of unit n in plant i [MW]
P_i^{\max}	Maximum power output of plant i [MW]
P_i^{\min}	Minimum power output of plant i [MW]
P_m^{Pr}	Rated power of unit m [MW]
$Q_{i,n}^{\max}$	Maximum turbine discharge of unit n in plant i [m ³ /s]
$Q_{i,n}^{\min}$	Minimum turbine discharge of unit n in plant i [m ³ /s]
Q_i^{\max}	Maximum total water discharge of plant i [m ³ /s]
Q_i^{\min}	Minimum total water discharge of plant i [m ³ /s]
Q_m^{\max}	Maximum pumped flow of unit m in the pumping station [m ³ /s]
Q_m^{\min}	Minimum pumped flow of unit m in the pumping station [m ³ /s]
$R_{s,t}$	Solar radiation intensity [W/m ²]
t_e	Minimum number of continuous periods of the unit n
T_{cref}	Temperature under standard test conditions (25 °C)
$T_{i,n}^{\text{off}}$	Minimum required offline duration of unit n in plant i [15 min]
$T_{i,n}^{\text{on}}$	Minimum required online duration of unit n in plant i [15 min]
$Z_{i,\text{begin}}^{\text{up}}$	Initial water level of reservoir i [m]
$Z_{i,\text{end}}^{\text{up}}$	Target water level of reservoir i at the end of the scheduling horizon [m]
$Z_i^{\text{up,max}}$	Upper bound of the forebay water level of reservoir i [m]
$Z_i^{\text{up,min}}$	Lower bound of the forebay water level of reservoir i [m]
C_p	Wind energy utilization coefficient
P_e	Rated power of wind farms [MW]
$R_{i,t}$	Forecasted local reservoir inflow of plant i in time period t [m ³ /s]
V_i, V_r, V_o	Cut-in, rated, and cut-off wind speeds [m/s]
Variables	
$Z_{i,t}^{\text{down}}$	Tailwater level of reservoir i in time period t [m]
$u_{i,n,t}$	Binary variable that is equal to 1 if unit n is online in time period t , but is otherwise equal to 0
$u_{m,t}$	Binary variable that is equal to 1 if unit m is online in time period t , but is otherwise equal to 0
f_1, f_2, f_3	Objective functions
$H_{i,n,t}^{\text{loss}}$	Head loss of the unit n in plant i in time period t [m]
$H_{i,n,t}$	Net water head of unit n in plant i in time period t [m]
$H_{m,t}$	Pumping head of unit m in time period t [m]
P_t^H	Power output of the hydropower plant in time period t [MW]
$P_t^{\text{PV,C}}$	Energy curtailment of the solar power station in time period t [MW]
P_t^{PV}	Power output of solar power station in time period t [MW]
$P_t^{\text{W,C}}$	Energy curtailment of the wind farm in time period t [MW]
P_t^W	Power output of the wind farm in time period t [MW]
P_{av}	Net load average value of the scheduling period [MW]
$P_{i,n,t}$	Power output of unit n in plant i in time period t [MW]
$P_{i,t}$	Power output of hydropower plant i in time period t [MW]
$P_{m,t}$	Power consumption of pump unit m in time period t [MW]
P_{nt}	Net load of the system in time period t [MW]
P_t^P	Power consumption of the pumping station in time period t [MW]

Q_t^p	Total pumping flow of the pumping station in time period t [m^3/s]
$Q_{i,n,t}$	Generating water flow of unit n in plant i in time period t [m^3/s]
$Q_{i,t}^d$	Total water spillage of plant i in time period t [m^3/s]
$Q_{i,t}^p$	Generating water flow of plant i in time period t [m^3/s]
$Q_{m,t}$	Pumping flow of pump unit m in time period t [m^3/s]
T_t	Actual temperature of the cell in the period [$^\circ\text{C}$]
$y_{i,n,t}^{\text{off}}$	Binary variable that equals 1 if unit n is shut down in time period t , but otherwise equals 0
$y_{i,n,t}^{\text{on}}$	Binary variable that equals 1 if unit n is started up in time period t , but otherwise equals 0
$Z_{i,t}^{\text{up}}$	Forebay water level of reservoir i in time period t [m]
$I_{i,t}$	Reservoir total inflow of plant i in time period t [m^3/s]
$Q_{i,t}$	Total outflow of plant i in time period t [m^3/s]
V_t	Actual wind speed [m/s]
$V_{i,t}$	Reservoir water storage of plant i at the end of time period t [m^3]
Functions	
$f_i^{\text{zq}}(\cdot)$	Relation function between the tailwater level and total water discharge of plant i
$f_{i,n}^{\text{HQ}}$	Relation function between head loss and turbine flow of unit n in plant i
$f_i^{\text{zv}}(\cdot)$	Relation function between the forebay water level and water storage of plant i
$f_m^p(\cdot)$	Relation function between the power consumption, net water head, and pumped flow of unit m
$f_{i,n}^h(\cdot)$	Relation function between the power production, net water head, and generating water flow of unit n in plant i

References

- Wang, C.; Liu, C.; Chen, J.; Zhang, G. Cooperative planning of renewable energy generation and multi-timescale flexible resources in active distribution networks. *Appl. Energy* **2024**, *356*, 122429. [[CrossRef](#)]
- Sun, Y.; Li, Y.; Wang, R.; Ma, R. Assessing the national synergy potential of onshore and offshore renewable energy from the perspective of resources dynamic and complementarity. *Energy* **2023**, *279*, 128106. [[CrossRef](#)]
- Yu, S.; Wan, K.; Cai, C.; Xu, L.; Zhao, T. Resource curse and green growth in China: Role of energy transitions under COP26 declarations. *Resour. Policy* **2023**, *85*, 103768. [[CrossRef](#)]
- Chen, C.; Liu, H.; Xiao, Y.; Zhu, F.; Ding, L.; Yang, F. Power Generation Scheduling for a Hydro-Wind-Solar Hybrid System: A Systematic Survey and Prospect. *Energies* **2022**, *15*, 8747. [[CrossRef](#)]
- Javed, M.S.; Ma, T.; Jurasz, J.; Amin, M.Y. Solar and wind power generation systems with pumped hydro storage: Review and future perspectives. *Renew. Energy* **2020**, *148*, 176–192. [[CrossRef](#)]
- Schmidt, J.; Cancelli, R.; Junior, A.O.P. The effect of windpower on long-term variability of combined hydro-wind resources: The case of Brazil. *Renew. Sust. Energy Rev.* **2016**, *55*, 131–141. [[CrossRef](#)]
- Weschenfelder, F.; Leite, G.D.N.P.; Costa, A.C.A.D.; Vilela, O.D.C.; Ribeiro, C.M.; Ochoa, A.A.V.; Araújo, A.M. A review on the complementarity between grid-connected solar and wind power systems. *J. Clean. Prod.* **2020**, *257*, 120617. [[CrossRef](#)]
- Zhang, H.; Lu, Z.; Hu, W.; Wang, Y.; Dong, L.; Zhang, J.T. Coordinated optimal operation of hydro-wind-solar integrated systems. *Appl. Energy* **2019**, *242*, 883–896. [[CrossRef](#)]
- Lu, N.; Wang, G.; Su, C.; Ren, Z.; Peng, X.; Sui, Q. Medium-and long-term interval optimal scheduling of cascade hydropower-photovoltaic complementary systems considering multiple uncertainties. *Appl. Energy* **2024**, *353*, 122085. [[CrossRef](#)]
- Jin, X.; Liu, B.; Liao, S.; Cheng, C.; Li, G.; Liu, L. Impacts of different wind and solar power penetrations on cascade hydroplants operation. *Renew. Energy* **2022**, *182*, 227–244. [[CrossRef](#)]
- Tan, Q.; Nie, Z.; Wen, X.; Su, H.; Fang, G.; Zhang, Z. Complementary scheduling rules for hybrid pumped storage hydropower-photovoltaic power system reconstructing from conventional cascade hydropower stations. *Appl. Energy* **2024**, *355*, 122250. [[CrossRef](#)]
- Li, H.; Zhang, R.; Mahmud, M.A.; Hredzak, B. A novel coordinated optimization strategy for high utilization of renewable energy sources and reduction of coal costs and emissions in hybrid hydro-thermal-wind power systems. *Appl. Energy* **2022**, *320*, 119019. [[CrossRef](#)]
- Yuan, W.; Zhang, S.; Su, C.; Wu, Y.; Yan, D.; Wu, Z. Optimal scheduling of cascade hydropower plants in a portfolio electricity market considering the dynamic water delay. *Energy* **2022**, *252*, 124025. [[CrossRef](#)]
- Su, C.; Wang, P.; Yuan, W.; Wu, Y.; Jiang, F.; Wu, Z.; Yan, D. Short-term optimal scheduling of cascade hydropower plants with reverse-regulating effects. *Renew. Energy* **2022**, *199*, 395–406. [[CrossRef](#)]

15. Zhang, Y.; Cheng, C.T.; Cai, H.; Jin, X.; Jia, Z.B.; Wu, X.; Su, H.; Yang, T. Long-term stochastic model predictive control and efficiency assessment for hydro-wind-solar renewable energy supply system. *Appl. Energy* **2022**, *316*, 119134. [[CrossRef](#)]
16. Guo, Y.; Ming, B.; Huang, Q.; Wang, Y.; Zheng, X.; Zhang, W. Risk-averse day-ahead generation scheduling of hydro-wind-photovoltaic complementary systems considering the steady requirement of power delivery. *Appl. Energy* **2022**, *309*, 118467. [[CrossRef](#)]
17. Ren, Y.; Yao, X.; Liu, D.; Qiao, R.; Zhang, L.; Zhang, K.; Jin, K.; Li, H.; Ran, Y.; Li, F. Optimal design of hydro-wind-PV multi-energy complementary systems considering smooth power output. *Sustain. Energy Technol. Assess.* **2022**, *50*, 101832. [[CrossRef](#)]
18. Zhang, Z.; Qin, H.; Li, J.; Liu, Y.; Yao, L.; Wang, Y.; Wang, C.; Pei, S.; Zhou, J.Z. Short-term optimal operation of wind-solar-hydro hybrid system considering uncertainties. *Energy Convers. Manag.* **2020**, *205*, 112405. [[CrossRef](#)]
19. Tan, Q.; Wen, X.; Sun, Y.; Lei, X.; Wang, Z.; Qin, G. Evaluation of the risk and benefit of the complementary operation of the large wind-photovoltaic-hydropower system considering forecast uncertainty. *Appl. Energy* **2021**, *285*, 116442. [[CrossRef](#)]
20. Shi, X.; Jia, R.; Huang, Q.; Huang, G.; Lei, X.; Li, J.; Ming, B.; Zhao, Z.; Li, L. Day-ahead complementary operation for wind-hydro-thermal system considering the multi-dimensional uncertainty. *Csee J. Power Energy Syst.* **2022**, *1*–11. [[CrossRef](#)]
21. Liao, S.; Liu, H.; Liu, B.; Zhao, H.; Wang, M. An information gap decision theory-based decision-making model for complementary operation of hydro-wind-solar system considering wind and solar output uncertainties. *J. Clean. Prod.* **2022**, *348*, 131382. [[CrossRef](#)]
22. Huang, K.; Liu, P.; Kim, J.S.; Xu, W.; Gong, Y.; Cheng, Q.; Zhou, Y. A model coupling current non-adjustable, coming adjustable and remaining stages for daily generation scheduling of a wind-solar-hydro complementary system. *Energy* **2023**, *263*, 125737. [[CrossRef](#)]
23. Jiang, W.; Liu, Y.; Fang, G.; Ding, Z. Research on short-term optimal scheduling of hydro-wind-solar multi-energy power system based on deep reinforcement learning. *J. Clean. Prod.* **2023**, *385*, 135704. [[CrossRef](#)]
24. Xie, J.; Zheng, Y.; Pan, X.; Zheng, Y.; Zhang, L.; Zhan, Y. A short-term optimal scheduling model for wind-solar-hydro hybrid generation system with Cascade hydropower considering regulation reserve and spinning reserve requirements. *IEEE Access* **2021**, *9*, 10765–10777. [[CrossRef](#)]
25. Huang, K.; Liu, P.; Ming, B.; Kim, J.S.; Gong, Y. Economic operation of a wind-solar-hydro complementary system considering risks of output shortage, power curtailment and spilled water. *Appl. Energy* **2021**, *290*, 116805. [[CrossRef](#)]
26. Shu, S.; Mo, L.; Wang, Y. Peak shaving strategy of wind-solar-hydro hybrid generation system based on modified differential evolution algorithm. *Energy Procedia* **2019**, *158*, 3500–3505. [[CrossRef](#)]
27. Li, J.; Lu, J.; Yao, L.; Cheng, L.; Qin, H. Wind-solar-hydro power optimal scheduling model based on multi-objective dragonfly algorithm. *Energy Procedia* **2019**, *158*, 6217–6224. [[CrossRef](#)]
28. Zhang, Q.; Xie, J.; Pan, X.; Zhang, L.; Fu, D. A short-term optimal scheduling model for wind-solar-hydro-thermal complementary generation system considering dynamic frequency response. *IEEE Access* **2021**, *9*, 142768–142781. [[CrossRef](#)]
29. Liu, B.; Liu, T.; Liao, S.; Lu, J.; Cheng, C.T. Short-term coordinated hybrid hydro-wind-solar optimal scheduling model considering multistage section restrictions. *Renew. Energy* **2023**, *217*, 119160. [[CrossRef](#)]
30. Tan, S.; Wang, X.; Jiang, C. Optimal scheduling of hydro-PV-wind hybrid system considering CHP and BESS coordination. *Appl. Sci.* **2019**, *9*, 892. [[CrossRef](#)]
31. Wang, Q.; Luo, X.; Gong, N.; Ma, H. Day-ahead optimal dispatching of wind-solar-hydro-thermal combined power system with pumped-storage hydropower integration. In Proceedings of the 2018 IEEE Innovative Smart Grid Technologies-Asia (ISGT Asia), Singapore, 22–25 May 2018; pp. 430–434.
32. Zhang, T.; Huang, W.; Chen, S.; Zhu, Y.; Kang, F.; Zhou, Y.; Ma, G. The scheduling research of a wind-solar-hydro hybrid system based on a sand-table deduction model at ultra-short-term scales. *Energies* **2023**, *16*, 3280. [[CrossRef](#)]
33. Guo, S.; Zheng, K.; He, Y.; Kurban, A. The artificial intelligence-assisted short-term optimal scheduling of cascade hydro-photovoltaic complementary system with hybrid time steps. *Renew. Energy* **2023**, *202*, 1169–1189. [[CrossRef](#)]
34. Ak, M.; Kentel, E.; Savasaneril, S. Quantifying the revenue gain of operating a cascade hydropower plant system as a pumped-storage hydropower system. *Renew. Energy* **2019**, *139*, 739–752. [[CrossRef](#)]
35. Jurasz, J.; Mikulik, J.; Krzywda, M.; Ciapała, B.; Janowski, M. Integrating a wind- and solar-powered hybrid to the power system by coupling it with a hydroelectric power station with pumping installation. *Energy* **2018**, *144*, 549–563. [[CrossRef](#)]
36. Xu, X.; Hu, W.; Cao, D.; Huang, Q.; Chen, C.; Chen, Z. Optimized sizing of a standalone PV-wind-hydropower station with pumped-storage installation hybrid energy system. *Renew. Energy* **2020**, *147*, 1418–1431. [[CrossRef](#)]
37. Zhang, J.; Cheng, C.; Yu, S.; Shen, J.; Wu, X.; Su, H. Preliminary feasibility analysis for remaking the function of cascade hydropower stations to enhance hydropower flexibility: A case study in China. *Energy* **2022**, *260*, 125163. [[CrossRef](#)]
38. Wang, Z.; Fang, G.; Wen, X.; Tan, Q.; Zhang, P.; Liu, Z. Coordinated operation of conventional hydropower plants as hybrid pumped storage hydropower with wind and photovoltaic plants. *Energy Convers. Manag.* **2023**, *277*, 16654. [[CrossRef](#)]
39. Ju, C.; Ding, T.; Jia, W.; Mu, C.; Zhang, H.; Sun, Y. Two-stage robust unit commitment with the cascade hydropower stations retrofitted with pump stations. *Appl. Energy* **2023**, *334*, 120675. [[CrossRef](#)]

40. Tang, Y.; Fang, G.; Tan, Q.; Wen, X.; Lei, X.; Ding, Z. Optimizing the sizes of wind and photovoltaic power plants integrated into a hydropower station based on power output complementarity. *Energy Convers. Manag.* **2020**, *206*, 112465. [[CrossRef](#)]
41. Su, C.; Cheng, C.; Wang, P.; Shen, J.; Wu, X. Optimization model for long-distance integrated transmission of wind farms and pumped-storage hydropower plants. *Appl. Energy* **2019**, *242*, 285–293. [[CrossRef](#)]

Disclaimer/Publisher’s Note: The statements, opinions and data contained in all publications are solely those of the individual author(s) and contributor(s) and not of MDPI and/or the editor(s). MDPI and/or the editor(s) disclaim responsibility for any injury to people or property resulting from any ideas, methods, instructions or products referred to in the content.